Supplementary Information

Acquisition of the contractile phenotype of arterial smooth muscle cells depends on the miR-143/145 gene cluster

Thomas Boettger, Nadine Beetz, Sawa Kostin, Johanna Schneider, Marcus

Krüger, Lutz Hein & Thomas Braun

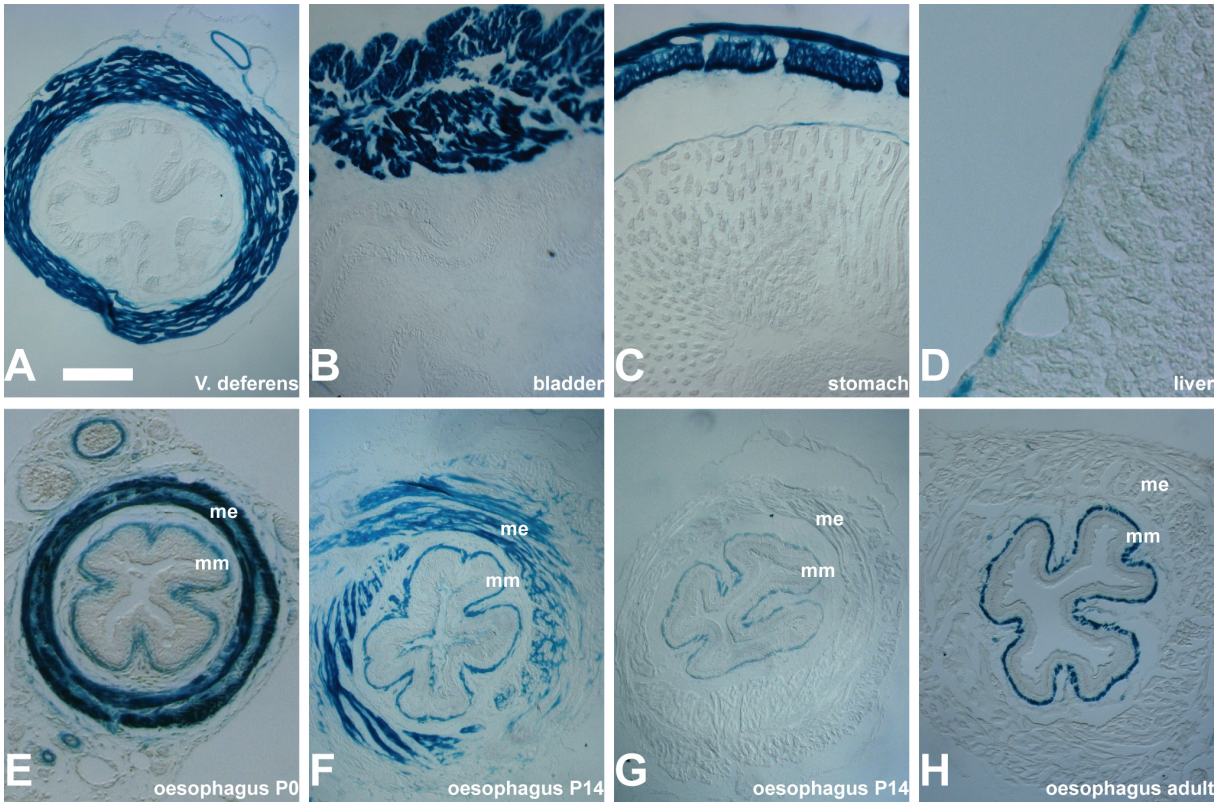

Supplementary Figure 1: The miR-143/145 locus is active in smooth muscle cells of all SMC-containing organs.

Expression of the LacZ reporter, which indicates activity of the miR-143/145 locus, was detected in all parts of the smooth muscle coat of the Vas deferens (A), in the smooth muscle layers of the adult bladder (B), and in the stomach (C). In the liver (D), a signal was found in smooth muscle cells of the ramifications of the portal vein. The expression of the miR-143/145 reporter in the oesophagus (E-H) follows the described expression of other smooth muscle genes: At P0 (E) the reporter was expressed in the muscularis mucosae (mm) and the muscularis externa (me). At P14, expression in the esophagus was detected in the muscularis mucosa. Expression in the muscularis externa at this stage was only found proximal (F) but not distal to the stomach (G) since the distal part of the muscularis externa contains skeletal muscle cells at this stage. In the adult esophagus lacZ staining was only found in the muscularis mucosa (H). Scale bar corresponds to 189 µm in A, B, C, F, G, H, 46 µm in D, 94 µm in E.

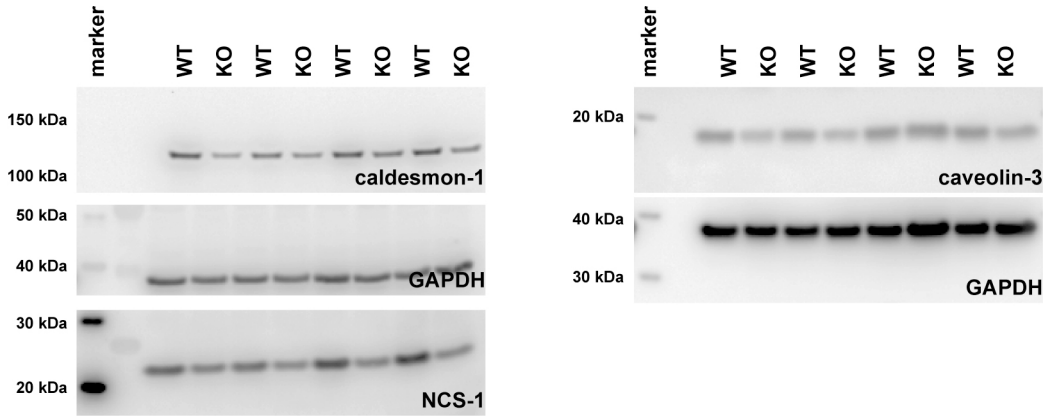

Supplementary Figure 2: The loss of mir-143/45 causes multiple secondary changes of protein expression.

Western blot analysis of caveolin-3, NCS-1 and caldesmon-1 expression in aortae of WT and miR-143/145 KO mice. Western blots were normalized to corresponding GAPDH signals. Please note the down-regulation of caveolin-3, NCS-1 and caldesmon-1 proteins, which were also found to be down-regulated in Affymetrix expression analysis. The GAPDH normalized ratio KO/WT was 0.7, 0.59 and 0.55 for caveolin-3, NCS-1 and caldesmon-1, respectively ($n=4/4$, $p<0.05$).

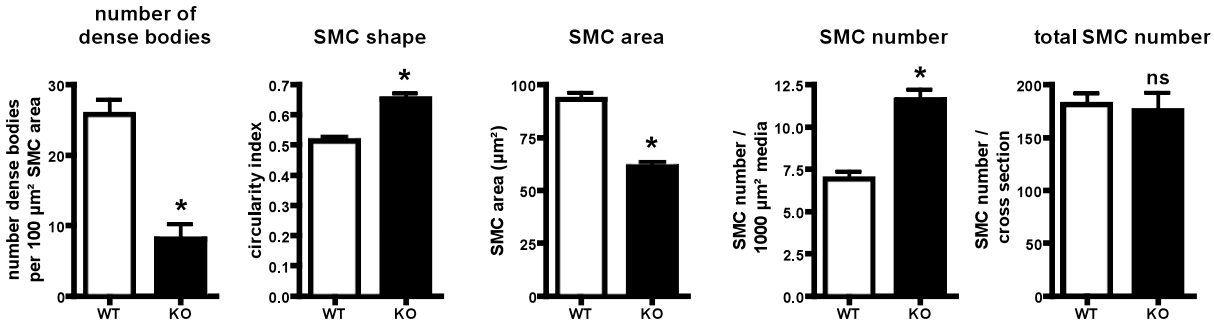

Supplementary Figure 3: Changes in morphological parameters reflecting the phenotypic switch of VSMCs from contractile to synthetic. Detailed morphometric analysis of VSMCs in the A. femoralis of KO and WT animals. A striking reduction in the number of dense bodies, which are essential to strengthen and support the contractile apparatus in VSMCs, was detected in KO animals (8.02 ± 2.19 in KO compared to 25.7 ± 2.13 in WT; mean ± SEM, n=3 for each genotype, p-value=0.0044 as determined by unpaired t-test). The VSMCs of KO mice were much more oval than those in WT (circularity index: 0.51 ± 0.01 in WT compared to 0.65 ± 0.02 in KO; mean ± SEM, n=3 for each genotype, p-value=0.0038 as determined by unpaired t-test). The shape of VSMCs (circularity index) was determined concomitantly with the area covered by VSMCs using the Image J program with at least 300 randomly selected cells per 3 transversally sectioned arterial segments (minimum 100 µm). The size of the VSMCs of the KO was reduced, the number of VSMC/area was increased, while the total cell number did not change significantly (Number of VSMC/cross section in WT 181 ± 11 compared to 175 ± 18 in KO mice; mean ± SEM, n=3 for each genotype, p-value=0.7848 as determined by unpaired t-test. VSMC area 92.78 ± 3.30 in WT compared to 61.23 ± 2.28 in KO; mean ± SEM, n=3 for each genotype, p-value=0.0014 as determined by unpaired t-test, Number of VSMC/1000 µm² media in WT 6.9 ± 0.4 compared to 11.6 ± 0.6; mean ± SEM, n=3 for each genotype, p-value=0.0037 as determined by unpaired t-test). Quantitative measurements support our conclusion that the decreased medial wall thickness is due to decreased cell size but not due to decreased total cell number. (* indicates significance $p<0.005$, n=3/3 animals). The data clearly indicate the switch from contractile to synthetic VSMCs.

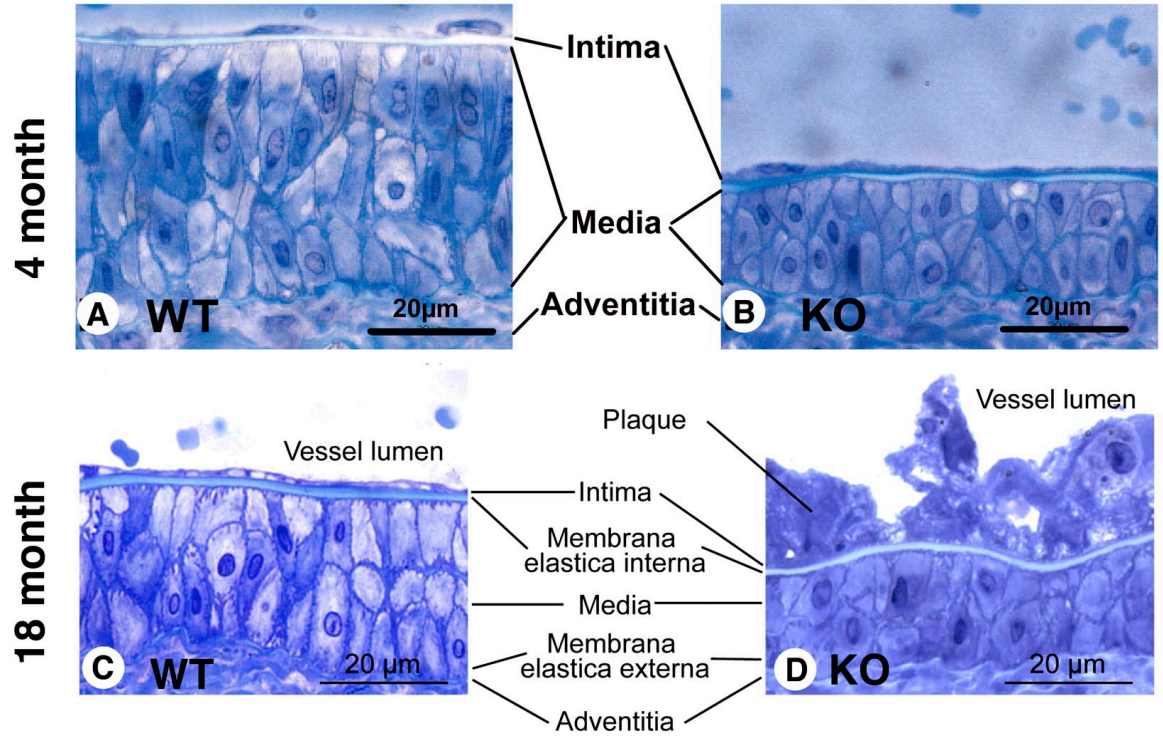

Supplementary Figure 4: Changes in the morphology of vessels walls of mutant mice at different ages. (A-B) Representative light microscopic images comparing the thickness of the media in WT and mutant vessel walls. Note the reduced cellular area of VSMCs and a decreased media thickness in mutant compared to WT mice. (C, D) Vessels of older mutant mice (18 month) did frequently contain neointimal lesions, which were never seen in WT mice.

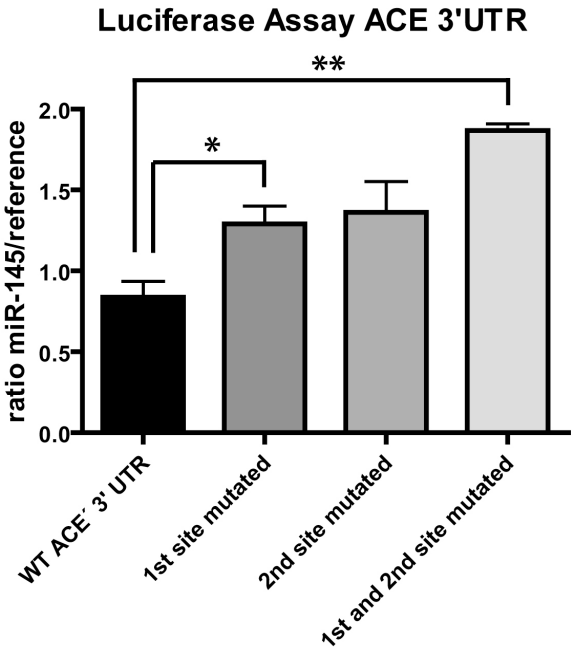

Supplementary Figure 5: miR-145 specifically reduces activity of a luciferase-reporter under the control of the ACE 3' UTR. Results of co-transfection experiments of a luciferase reporter plasmid carrying WT or mutated miR-145 bindings sites and a miR-145 expression vector in Hela-cells are shown. Higher luciferase activities, i.e. reduced repression by the co-transfected miR-145 plasmid was scored when reporter with mutations in the first or second miR-145 target or a combination of both were used. Changes were significant compared to the WT-vector (* $p<0.05$; ** $p<0.001$). A part of the ACE 3' UTR was PCR-amplified (GCTCGTGGCCACCGTGGGTCTCGCC, TAGGCCTTCCAAAGGATGGCTGA GG) and cloned into the XbaI site of pGL3 (Promega) immediately 3' of the luciferase ORF. Mutants of the UTR were constructed using mutated oligonucleotides and a two- or three step PCR. The first predicted miR-145 target site was mutated from GGAGTGTCCCATAAGAAACTGGA to GGAGTGTCCCATAAGAAAtgaaA. The second target site was mutated from GGGAAGCCAGGGACAGGA to GGGAAGCCAGGGACAttc and a vector with mutation of both sites was prepared. 50% confluent Hela-1 cells on 24-well plates were co-transfected using Lipofectamine 2000 (Invitrogen) with luciferase vectors (80 ng) together with a renilla vector (pRL-TK, Promega; 20 ng) with 167 nM mmu-mir-145 miRIDIAN Mimic or a control-miR (Thermo Scientific Dharmacon), respectively. Each transfection was done in triplicate. Cells were lysed after 48 h and luciferase and renilla activities were determined using the Dual-Luciferase® Reporter Assay (Promega) and a Mithras LB940 plate reader (Berthold Technologies). miR-145 ratios were normalized to the respective controls.

Protein Names	Symbol	ratio
Quinone oxidoreductase; Crystallin, zeta	Cryz	**9.2**
protein N-myristoyltransferase 1	Nmt1	**6.7**
CD166 antigen precursor	Alcam	**5.5**
collectin sub-family member 12	Colec12	**5.1**
Angiotensin-converting enzyme	**Ace**	**4.9**
Thiosulfate sulfurtransferase	Tst	**4.2**
Malic enzyme 1	Me1, Mod-1, Mod1	**3.8**
Adenosine kinase	Adk	**3.6**
myosin heavy chain 10, non-muscle	Myh10	**3.6**
FK506-binding protein 3	Fkbp3, Fkbp25	**3.4**
Ectonucleotide pyrophosphatase	Enpp1, Npps	**3.4**
Tubulin beta-4 chain	Tubb4	**3.3**
Tubulin beta-5 chain	Tubb5	**3.1**
Fatty acid-binding protein, heart	Fabp3, Fabph1	**3.1**
Versican core protein precursor	Vcan, Cspg2	**2.7**
Glia maturation factor beta	Gmfb	**2.7**
Protein disulfide-isomerase A3 precursor	Pdia3, Erp	**2.7**
Hyaluronan and proteoglycan link protein 1 precursor	Hapln1, Crtl1	**2.7**
Heat shock protein 90 kDa beta member 1	Hsp90b1, Tra-1	**2.6**
Epoxide hydrolase 2	Ephx2, Eph2	**2.6**
Stress-associated endoplasmic reticulum protein 2	Serp2, Ramp4	**2.5**
Ubiquitin carboxyl-terminal hydrolase 5	Usp5, Isot	**2.4**
Leukocyte elastase inhibitor A	Serpinb1a	**2.3**
Tropomyosin alpha-4 chain;Tropomyosin-4	**Tpm4**	**2.1**
Glutathione S-transferase	Gstm1, Gstm3	**2.1**
4F2 cell-surface antigen heavy chain	Slc3a2, Mdu1	**2.1**
Platelet-activating factor acetylhydrolase IB subunit beta	Pafah1b2	**2.0**
Insulin degrading enzyme	Ide	**2.0**
Microtubule-associated protein 1B	Map1b, Mtap5	**2.0**
Golgi integral membrane protein 4	Golim4	1.9
Enolase 3	Eno3	1.8
Hook homolog 3	Hook3	1.7
Nucleoside diphosphate kinase A	Nme1	1.7
CD31 antigen	Pecam1	1.7
Fibrinogen gamma chain precursor	Fgg	1.7
Spectrin alpha 2	Spna2	1.7
myosin regulatory light chain A, smooth muscle homolog;	2900073G15Rik	1.6
Elongation factor 2;EF-2	Eef2	1.6
Calnexin precursor	Canx	1.6
Aldose reductase homolog	2310005E10Rik	1.6
Glutathione S-transferase Mu 5	Gstm5	1.6

Supplementary Table 1 SILAC-detected proteins up-regulated in aortae miR-143/145 KO vs. WT.

A selection of proteins is shown that are detected to be significantly up-regulated in the SILAC experiment ($p<0.05$, n=3/3).

Protein Names	Symbol	ratio
ribosomal protein L7	Rpl7	**0.1**
Calcium/calmodulin-dependent protein kinase type II gamma chain	Camk2g	**0.1**
Tubulin polymerization-promoting protein family member 3	Tppp3	**0.2**
Eukaryotic translation initiation factor 2C 2;Argonaute-2;S	Eif2c2, Ago2	**0.3**
Melanoma-associated antigen MUC18;CD146 antigen	Mcam	**0.4**
Nuclear mitotic apparatus protein 1 homolog	Numa1	**0.4**
Serine/threonine-protein phosphatase PP1-beta catalytic subunit	Ppp1cb	**0.4**
protein kinase c delta-bindig protein homolog	Prkcdbp	**0.4**
Laminin subunit beta-2	Lamb2	**0.4**
Cytoglobin	Cygb	**0.4**
Smoothelin	Smtn	**0.4**
Laminin subunit gamma-1 precursor;Laminin B2 chain	Lamc1, Lamb-2	**0.4**
Histone H2A type 2-A	Hist2h2aa1	**0.4**
Glutamyl aminopeptidase;CD249 antigen	Enpep	**0.5**
Histone H4	Hist1h4a	**0.5**
Insulin-like growth factor-binding protein 7	Igfbp7, Mac25	**0.5**
Laminin subunit alpha-4 precursor	Lama4	**0.5**
CPI-17, Protein phosphatase 1 regulatory subunit 14A;17 kDa	Ppp1r14a, Cpi17	**0.5**
Heterogeneous nuclear ribonucleoprotein D-like	Hnrpdl	**0.5**
Voltage-dependent calcium channel subunit alpha-2/delta-1	Cacna2d1	**0.5**
Histone H2B type 1-H	Hist1h2bh	0.6
Calcium-binding protein 39	Cab39	0.6
MLCK Myosin light chain kinase, smooth muscle	Mylk	0.6
Tenascin X;Tenascin-X	Tnxb	0.6
CD81 antigen	Cd81	0.6
Clusterin precursor	Clu, Apoj	0.6
Integrin alpha-5 precursor	Itga5	0.6
Sodium/potassium-transporting ATPase subunit beta-3	Atp1b3	0.6
PDGF-associated protein	Pdap1	0.6
UNR-interacting protein	Strap, Unrip	0.6
NADPH-dependent carbonyl reductase	Dhrs4, D14Ucla2	0.6
Glycolipid transfer protein;GLTP	Gltp	0.6
Caveolin-2	Cav2	0.6

Supplementary Table 2: SILAC-detected proteins down-regulated in aortae miR-143/145 KO vs. WT.

A selection of proteins is shown, which was significantly down-regulated in the SILAC experiment ($p<0.05$, n=3/3). Selected markers of smooth muscle contraction are marked in red.

Probe Set ID	Gene Title	Gene Symbol	FC
1417464_at	troponin C2, fast	Tnnc2	5.57
1435354_at	potassium inwardly-rectifying channel, subfam. J, member 15	Kcnj15	5.13
1427735_a_at	actin, alpha 1, skeletal muscle	Acta1	4.74
1419608_a_at	melanoma inhibitory activity 1	Mia1	4.68
1416889_at	troponin I, skeletal, fast 2	Tnni2	4.24
1425425_a_at	Wnt inhibitory factor 1	Wif1	3.84
1448756_at	S100 calcium binding protein A9 (calgranulin B)	S100a9	3.48
1419312_at	ATPase, Ca++ transporting, cardiac muscle, fast twitch 1	Atp2a1/SERCA	3.36
1434411_at	collagen, type XII, alpha 1	Col12a1	3.27
1419473_a_at	Cholecystokinin	Cck	3.17
1419394_s_at	S100 calcium binding protein A8 (calgranulin A)	S100a8	3.16
1418480_at	pro-platelet basic protein	Ppbp	2.82
1448371_at	myosin light chain, phosphorylatable, fast skeletal muscle	Mylpf	2.75
1422926_at	melanocortin 2 receptor	Mc2r	2.68
1424525_at	gastrin releasing peptide	Grp	2.54
1437466_at	activated leukocyte cell adhesion molecule	Alcam	2.36
1449577_x_at	tropomyosin 2, beta	Tpm2	2.35
1423100_at	FBJ osteosarcoma oncogene	Fos	2.15
1450468_at	Myocilin	Myoc	2.13
1423062_at	insulin-like growth factor binding protein 3	Igfbp3	2.05
1419693_at	collectin sub-family member 12	Colec12	2.05
1433883_at	tropomyosin 4	Tpm4	2.02
1452661_at	transferrin receptor	Tfrc	1.99
1419871_at	Protein phosphatase 2 regulatory subunit A, beta isoform	Ppp2r1b	1.90
1449286_at	netrin G1	Ntng1	1.87
1418445_at	solute carrier family 16, member 2	Slc16a2	1.87
1425151_a_at	NADPH oxidase organizer 1	Noxo1	1.85
1429262_at	Ras association (RalGDS/AF-6) domain family member 6	Rassf6	1.83
1437401_at	insulin-like growth factor 1	Igf1	1.79
1420647_a_at	keratin 8	Krt8	1.78
1451912_a_at	fibroblast growth factor receptor-like 1	Fgfrl1	1.77
1433486_at	chloride channel 3	Clcn3	1.73
1427183_at	EGF-containing fibulin-like extracellular matrix protein 1	Efemp1	1.71
1452890_at	tubulin tyrosine ligase-like family, member 5	Ttll5	1.71
1433694_at	phosphodiesterase 3B, cGMP-inhibited	Pde3b	1.71
1438610_a_at	crystallin, zeta	Cryz	1.68
1447623_s_at	protein kinase D1	Prkd1	1.68
1438292_x_at	adenosine kinase	Adk	1.65
1435184_at	natriuretic peptide receptor 3	Npr3	1.61
1452398_at	phospholipase C, epsilon 1	Plce1	1.59
1451501_a_at	growth hormone receptor	Ghr	1.56
1448570_at	glia maturation factor, beta	Gmfb	1.47
1422208_a_at	guanine nucleotide binding protein (G protein), beta 5	Gnb5	1.45

Supplementary Table 3: Selected transcripts detected up-regulated in miR-143/145 KO vs. WT aortae.

A selection of transcripts, which was up-regulated in the Affymetrix GeneChip analysis, is shown ($p<0.05$, n=5/5; see methods). Selected signaling molecules, markers of smooth muscle contraction and of skeletal muscle differentiation are marked in yellow, red and blue, respectively.

Probe Set ID	Gene Title	Gene Symbol	FC
1417462_at	CAP, adenylate cyclase-associated protein 1 (yeast)	Cap1	0.14
1420942_s_at	regulator of G-protein signaling 5	Rgs5	0.23
1421698_a_at	collagen, type XIX, alpha 1	Col19a1	0.24
1449525_at	flavin containing monooxygenase 3	Fmo3	0.27
1437559_at	regulator of G-protein signalling 7 binding protein	Rgs7bp	0.27
1431167_at	diacylglycerol kinase, gamma	Dgkg	0.32
1446527_at	angiotensin II receptor, type 1b	Agtr1b	0.34
1437933_at	Hedgehog-interacting protein	Hhip	0.35
1417701_at	protein phosphatase 1, regulatory (inhibitor) subunit 14c	Ppp1r14c	0.37
1450389_s_at	phosphatidylinositol-4-phosphate 5-kinase, type 1 beta	Pip5k1b	0.39
1434887_at	frequenin homolog (Drosophila)	Freq	0.41
1449522_at	unc-5 homolog C (C. elegans)	Unc5c	0.41
1416286_at	regulator of G-protein signaling 4	Rgs4	0.42
1435720_at	potassium voltage-gated channel, Shal-related family, member 3	Kcnd3	0.42
1449876_at	protein kinase, cGMP-dependent, type I	Prkg1	0.45
1448598_at	matrix metallopeptidase 17	Mmp17	0.45
1460729_at	Rho-associated coiled-coil containing protein kinase 1	Rock1	0.45
1450700_at	CDC42 effector protein (Rho GTPase binding) 3	Cdc42ep3	0.47
1423635_at	bone morphogenetic protein 2	Bmp2	0.47
1455158_at	integrin alpha 3	Itga3	0.48
1435541_at	betacellulin, epidermal growth factor family member	Btc	0.49
1416357_a_at	melanoma cell adhesion molecule	Mcam	0.50
1424768_at	caldesmon 1	Cald1	0.50
1454159_a_at	insulin-like growth factor binding protein 2	Igfbp2	0.50
1423222_at	CAP, adenylate cyclase-associated protein, 2 (yeast)	Cap2	0.52
1433489_s_at	fibroblast growth factor receptor 2	Fgfr2	0.52
1430286_s_at	protein phosphatase 1, regulatory (inhibitor) subunit 14c	Ppp1r14c, CPI-17	0.54
1441042_at	fibroblast growth factor 1	Fgf1	0.54
1418413_at	caveolin 3	Cav3	0.54
1423585_at	insulin-like growth factor binding protein 7	Igfbp7	0.56
1452476_at	calcium channel, voltage-dependent, beta 2 subunit	Cacnb2	0.57
1423942_a_at	calcium/calmodulin-dependent protein kinase II gamma	Camk2g	0.58
1418744_s_at	similar to Tescalcin, tescalcin	Tesc	0.58
1416701_at	Rho family GTPase 3	Rnd3	0.58
1449660_s_at	coronin, actin binding protein 1C	Coro1c	0.60
1423049_a_at	tropomyosin 1, alpha	Tpm1	0.61
1424051_at	collagen, type IV, alpha 2	Col4a2	0.61
1422670_at	Rho family GTPase 2	Rnd2	0.62
1433682_at	Rho guanine nucleotide exchange factor (GEF) 17	Arhgef17	0.63
1423771_at	protein kinase C, delta binding protein	Prkcdbp	0.64
1419161_a_at	NADPH oxidase 4	Nox4	0.64
1424131_at	collagen, type VI, alpha 3	Col6a3	0.64
1417312_at	dickkopf homolog 3 (Xenopus laevis)	Dkk3	0.65
1437734_at	protein phosphatase 1, regulatory subunit 12A (Ppp1r12a)	MYPT1	0.66
1425506_at	myosin, light polypeptide kinase	Mylk	0.70

Supplementary Table 4: Selected transcripts detected down-regulated in miR-143/145 KO vs. WT aortae.

A selection of transcripts which was down-regulated in the Affymetrix GeneChip analysis is shown ($p<0.05$, n=5/5; see methods). Selected signaling molecules and markers of smooth muscle contraction are marked in yellow and red, respectively.

A) Selected target transcripts identified by Affymetrix GeneChip analysis

Gene Title	Symbol	p-value	FC	miRNA	database
Wnt inhibitory factor 1	Wif1	0.0095	3.8	miR-145	#
activated leukocyte cell adhesion molecule	**Alcam**	**0.0239**	**2.4**	**miR-145**	**#**
tropomyosin 4	**Tpm4**	**0.0002**	**2.0**	**miR-143, miR-145**	**#**
solute carrier family 16a2	Slc16a2	0.0015	1.9	miR-143, miR-145	#§
NADPH oxidase organizer 1	Noxo1	0.0162	1.8	miR-145	*
crystallin, zeta	**Cryz**	**0.0041**	**1.7**	**miR-143**	**#***
phospholipase C, epsilon 1	Plce1	0.0042	1.6	miR-145	*§
glia maturation factor, beta	**Gmfb**	**0.0002**	**1.5**	**miR-145**	**#§**
Rho GTPase activating protein 12	Arhgap12	0.0150	1.5	miR-145	#
FK506 binding protein 3	**Fkbp3**	**0.0041**	**1.3**	**miR-145**	**#*§**

B) Target proteins identified by SILAC analysis of protein expression

Gene Title	Symbol	p-value	ratio	miRNA	database
crystallin, zeta	**Cryz**	**0.0271**	**9.2**	**miR-143**	**#***
N-myristoyltransferase	Nmt1	0.0049	6.7	miR-143	§
activated leukocyte cell adhesion molecule	**Alcam**	**0.0351**	**5.5**	**miR-145**	**#**
Angiotensin-converting enzyme	Ace	0.0074	4.9	miR-145	*
myosin, heavy polypeptide 10, non-muscle	Myh10	0.0108	3.6	miR-143	#
FK506 binding protein 3	**Fkbp3**	**0.0430**	**3.4**	**miR-145**	**#*§**
Type I phosphodiesterase	NPP1	0.0025	3.4	miR-143, miR-145	#
Versican core protein	Vcan	0.0291	2.7	miR-143	#*
glia maturation factor, beta	**Gmfb**	**0.0024**	**2.7**	**miR-145**	**#§**
Ubiquitin specific peptidase 5	Usp5	0.0153	2.4	miR-145	#
Tropomyosin 4	**Tpm4**	**0.0466**	**2.1**	**miR-143, miR-145**	**#**
Platelet-activating factor acetylhydrolase IB beta	Pafah1b2	0.0252	2.0	miR-143, miR-145	#
Microtubule-associated protein 1B	Map1b	0.0217	2.0	miR-143	#§
Platelet endothelial cell adhesion molecule	Pecam1	0.0392	1.7	miR-145	#

Supplementary Table 5: Analysis of mRNA und protein expression in miR-143/145 knockout mice and identification of target proteins.

(A) Transcriptional profiling of aortae from miR-143/145 knockout in comparison to WT mice (n=5/5) using Affymetrix GeneChip® Mouse Genome 430 2.0 arrays. Arrays were analyzed using the RMA algorithm. An unpaired t-test was performed for significance analysis. Fold changes and p-values are shown. (B) Quantitative comparative proteome analysis of protein extracts isolated from knockout and wild-type mouse aortae (n=3/3). Wild-type mice completely labeled with the 13C6Lys-substituted version of lysine (”SILAC mice”) were used as a reference. Ratios of detected proteins were calculated using the maxquant 11.5 software. Ratios and p-values were calculated from the mean of three 13C6Lys-WT/WT and three 13C6Lys-WT/KO ratios. Lists of significantly up-regulated molecules were compared to predicted targets of mir-143 and miR-145 using the matchminer tool (18). Targets detected to be up-regulated by both unbiased screens at transcript- and protein level are in bold print; *, #, § label targets predicted by miRBase, miRNA.org or TargetScan, respectively.